Spin accumulation on a one-dimensional mesoscopic Rashba ring

2006 J. Phys.: Condens. Matter 18 4101

(http://iopscience.iop.org/0953-8984/18/16/017)

INSTITUTE OF PHYSICS PUBLISHING JOURNAL OF PHYSICS: CONDENSED MATTER

J. Phys.: Condens. Matter **18** (2006) 4101–4109 doi:10.1088/0953-8984/18/16/017

Spin accumulation on a one-dimensional mesoscopic Rashba ring

Zhi-Yong Zhang

Department of Physics, Nanjing University, Nanjing 210093, People's Republic of China

Received 6 December 2005
Published 7 April 2006
Online at stacks.iop.org/JPhysCM/18/4101

Abstract

The nonequilibrium spin accumulation on a one-dimensional (1D) mesoscopic Rashba ring is investigated with unpolarized current injected through ideal leads. Due to the Rashba spin–orbit (SO) coupling and back-scattering at the interfaces between the leads and the ring, a beating pattern is formed in the fast oscillation of spin accumulation. If every beating period is complete, a plateau is formed, where the variation of spin accumulation with the external voltage is slow, but if new incomplete periods emerge in the envelope function, a transitional region appears. This plateau structure and the beating pattern are related to the tunnelling through spin-dependent resonant states. Because of the Aharonov–Casher (AC) effect, the average spin accumulation oscillates quasi-periodically with the Rashba SO coupling and has a series of zeros. In some situations, the direction of the average spin accumulation can be reversed by the external voltage in this 1D Rashba ring.

1. Introduction

Because of the development of semiconductor spintronics [1–3], the spin Hall effect [4–7] induced by the spin–orbit (SO) coupling in semiconductors has attracted a lot of interest. A two-dimensional electronic gas (2DEG) with Rashba SO coupling, [8] arising from the inversion asymmetry of the confining electric potential, is

$$H = \frac{\vec{p}^2}{2m^*} + \frac{\alpha}{\hbar}(\hat{\vec{\tau}} \times \vec{p}) \cdot \vec{z} + V_{\text{conf}}(x, y), \tag{1}$$

with $\hat{\vec{\tau}}$ the Pauli operator, α the Rashba SO coupling and V_{conf} the confining potential. As in the classical Hall effect, where electrons flowing along a conductor are subjected to a transverse Lorentz force caused by a perpendicular magnetic field and are separated in the transverse direction according to their charges, a longitudinal spin current along a 2DEG with SO coupling is subjected to a spin transverse 'force' [9, 10], which can be extracted within the Heisenberg picture as $\vec{f} = \frac{2\alpha^2 m^*}{\hbar^3}(\vec{p} \times \vec{z})\hat{\tau}^z - \vec{\nabla} V_{\text{conf}}(x, y)$. This spin transverse 'force' depends on spin and has no classic counterpart, and its physical meaning is contained in the quantum-mechanical

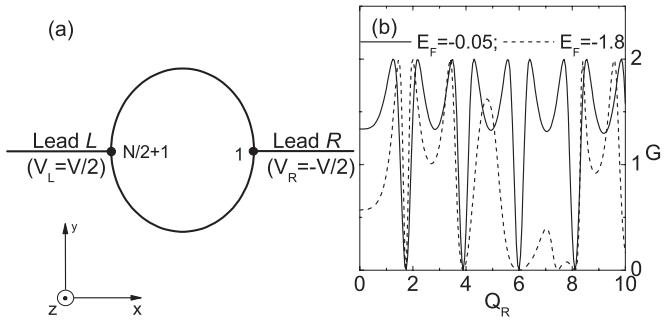

Figure 1. (a) Schematic illustration of the structure. (b) G–Q_{R} curves at $E_{\mathrm{F}} = -0.05$ (solid) and -1.8 (dashed) with $t = t_{\mathrm{L}} = 1$, $V = 0$ and $N = 100$.

expectation value. The direction of this 'force' depends on the electronic spin polarized on the z-axis, and oscillates on the scale of the spin precession length $L_{\mathrm{SO}} = \frac{\pi\hbar^2}{2m^*\alpha}$ because $|\uparrow\rangle$ and $|\downarrow\rangle$ are not the eigenstates of the system. With unpolarized charge current flowing through a finite-size 2DEG with Rashba SO coupling, spin-$\uparrow$ and spin-$\downarrow$ electrons can be separated and accumulated on the opposite lateral edges, which has been confirmed in the recent optical detection experiments [11, 12] and analysed in theory intensively [13–18]. If ideal transverse leads (without SO coupling) are attached to the structures, a pure spin transverse current may appear [19–21].

If V_{conf} confines the 2DEG to a mesoscopic ring [22], according to the formula of the spin transverse 'force', in a 1D isolated ring, $\vec{f}$ is perpendicular to the perimeter everywhere, and electrons with different spin directions cannot be separated. But as an electron is incident through an ideal lead into the ring, the scattering at the interface splits the wavefunction into two parts. Although the 'forces' on the two split waves are both perpendicular to the perimeter, the 'composite force' is transverse to the longitudinal unpolarized charge current and the spin accumulation in this open system becomes possible only if the coherence between the two split parts is kept. In the 1D mesoscopic Rashba ring, the spin-sensitive quantum interference caused by the difference in the Aharonov–Casher (AC) phase [23, 24] plays an important role in electronic transport [25–29], and so does the back-scattering at interfaces between the leads and the ring, which modulate the electronic wavefunctions. Obviously, these factors will influence the spin accumulation. The purpose of the present paper is to clarify the special properties of the spin accumulation in this 1D mesoscopic Rashba ring and the influences of the AC effect and the back-scattering at the interfaces.

For this purpose, we consider a structure schematically illustrated in figure 1(a), and study the properties of spin accumulation in the nonequilibrium ballistic transport process by assuming that the structural dimension is much smaller than the coherence length. Here, we only numerically calculate the nonequilibrium charge current J and the spin accumulation S^z, but do not give an analytical expression of $\vec{f}$ because it is difficult to obtain this expression for a hybrid structure and, more importantly, because $\vec{f}$ is not a measurable variable in experiments. Due to the spin Hall effect and back-scattering at the interfaces between the leads and the ring, a beating pattern is formed in the variation of S^z with the ring site n, and the fast oscillation of S^z–n curve is modulated by a slow one. If every beating period in the envelope function is complete, a plateau can be found, where the variations of J and the S^z–n curve with the external voltage V are slow. In a transitional region between two successive plateaus, new incomplete beating periods appear. This plateau structure and the beating pattern are both related to the tunnelling through spin-dependent resonant peaks and if every resonant peak

appearing in the nonequilibrium transmission window is complete, a plateau is formed. Due to the AC effect, J and the average spin accumulation $\langle S^z\rangle$ oscillate quasi-periodically with the Rashba SO coupling and exhibit a series of zeros at the same positions. In some situations, the direction of $\langle S^z\rangle$ can be reversed by V in this ring structure.

The organization of this paper is as follows. In section 2, the theoretical model and calculation method are presented. In section 3, the numerical results are illustrated and discussed. A brief summary is given in section 4.

2. Model and formulae

In the present paper, we consider the ballistic transport through a 1D mesoscopic Rashba ring and investigate the nonequilibrium spin accumulation on the ring when unpolarized charge current is injected through ideal leads. Our attention is focused on the influences of back-scattering at the interfaces between the leads and the ring and the AC effect resulting from electronic spin precession along the arms of ring caused by the Rashba SO coupling. The structure considered is schematically illustrated in figure 1(a), where a mesoscopic ring of length N with the SO hopping parameter $t_{\rm SO}$ is connected to two ideal leads where no SO interaction exists. In the present paper, we only consider a structure where the two leads are connected symmetrically to the ring with the same tunnelling matrix element $t_{\rm L}$. With external voltage applied, the chemical potentials of the two leads become $\mu_l = V_l$ with $l = {\rm L}, {\rm R}$ and the system is generally in the nonequilibrium state unless $V_{\rm L} = V_{\rm R}$. Without loss of generality, it is assumed that $V_{\rm L} = -V_{\rm R} = V/2$ with the chemical potential of the ring set as zero. With the z direction perpendicular to the ring plane, the Hamiltonian of the system including the ring and leads can be written in the tight-binding representation as [22, 28, 29]

$$H = H_{\rm ring} + H_{\rm L} + H_{\rm R} + H_{\rm T}, \tag{2}$$

where $H_{\rm ring}$, H_l and $H_{\rm T}$ are the Hamiltonians of the ring, the leads and the tunnelling between them. They are

$$H_{\rm ring} = \sum_{n=1\sigma}^{N}\left\{-t d^{\dagger}_{n\sigma} d_{n+1\sigma} + {\rm i}t_{\rm SO}\sum_{\sigma'}(\cos\varphi_n \hat{\tau}^x_{\sigma\sigma'} + \sin\varphi_n \hat{\tau}^y_{\sigma\sigma\prime}) d^{\dagger}_{n\sigma} d_{n+1\sigma'} + {\rm H.c.}\right\}, \tag{3}$$

$$H_{\rm L} = \sum_{n=-\infty}^{-1}\sum_{\sigma}\left\{\frac{V}{2} c^{\dagger}_{n\sigma} c_{n\sigma} - t\left(c^{\dagger}_{n\sigma} c_{n-1\sigma} + {\rm H.c.}\right)\right\}, \tag{4}$$

$$H_{\rm R} = \sum_{n=1}^{\infty}\sum_{\sigma}\left\{-\frac{V}{2} c^{\dagger}_{n\sigma} c_{n\sigma} - t\left(c^{\dagger}_{n\sigma} c_{n+1\sigma} + {\rm H.c.}\right)\right\} \tag{5}$$

and

$$H_{\rm T} = -t_{\rm L}\sum_{\sigma}\left(c^{\dagger}_{-1\sigma} d_{N/2+1\sigma} + c^{\dagger}_{1\sigma} d_{1\sigma} + {\rm H.c.}\right), \tag{6}$$

where $d_{n\sigma}$ and $c_{n\sigma}$ are the electronic annihilation operators on the ring and leads, with $\sigma = \uparrow, \downarrow$. Here, $d_{N+1\sigma} = d_{1\sigma}$, $\varphi_n = 2\pi(n - \frac{1}{2})/N$. With the z axis set as the quantization direction, $\hat{\tau}^x = \begin{pmatrix} 0 & 1 \\ 1 & 0 \end{pmatrix}$, $\hat{\tau}^y = \begin{pmatrix} 0 & -{\rm i} \\ {\rm i} & 0 \end{pmatrix}$ and $\hat{\tau}^z = \begin{pmatrix} 1 & 0 \\ 0 & -1 \end{pmatrix}$. This tight-binding Hamiltonian is obtained from the effective mass Hamiltonian (1) by employing the local orbital basis and has been successfully applied to quasi-1D and 2D structures with the spin Hall effect [17, 20, 28, 29]. It is related to the effective mass Hamiltonian (1) via the relations $t = \hbar^2/(2m^* a^2)$ and $t_{\rm SO} = \alpha/(2a)$ with a the lattice spacing.

Without external voltage $V = 0$, the system is in the equilibrium state and $\mu_l = 0$. When an electron on the Fermi surface $E_{\rm F}$ with spin σ is incident from the left lead to the

ring, the corresponding wavefunction in this lead is $\Psi_\sigma^{(\mathrm{inc})} = \sum_{n=-\infty}^{-1} \mathrm{e}^{\mathrm{i}k_\mathrm{L}n} c_{n\sigma}^\dagger |0\rangle$, with $|0\rangle$ the vacuum state. Similarly, the transmitted wavefunctions through the right lead can be written as $\Psi_\sigma^{(\mathrm{tr})} = \sum_{\sigma'} t_{\sigma',\sigma} \sum_{n=1}^{\infty} \mathrm{e}^{\mathrm{i}k_\mathrm{R}n} c_{n\sigma'}^\dagger |0\rangle$. Here, $-2t\cos k_l = E_\mathrm{F}$ in the two leads with $k_\mathrm{L} = k_\mathrm{R}$. The corresponding reflected wavefunction in the left lead is $\Psi_\sigma^{(r)} = \sum_{\sigma'} r_{\sigma',\sigma} \sum_{n=-\infty}^{-1} \mathrm{e}^{-\mathrm{i}k_\mathrm{L}n} c_{n\sigma'}^\dagger |0\rangle$. If the electronic wavefunction in the ring is expressed as $\Psi_\sigma = \sum_{n=1\sigma'}^{N} a_{n\sigma',\sigma} d_{n\sigma'}^\dagger |0\rangle$, the transmission coefficient $|t_{\sigma',\sigma}|^2$ through spin channel σ' and the electronic occupation probability $|a_{n\sigma',\sigma}|^2$ of spin σ' on the ring site n can be obtained by directly solving the Schrödinger equation. The conductance is

$$G = \sum_{\sigma',\sigma} |t_{\sigma',\sigma}|^2. \tag{7}$$

In the present paper, we only consider the situation at zero temperature. By this method, the influences of the interface scattering and the AC effect are taken into account. Without external magnetic flux, the Kramers degeneracy guarantees that $|t_{\sigma',\sigma}|^2$ is independent of the spin direction of the incident electron, and we can simply write the transmission coefficient as $|t_{\sigma'}|^2$. But if the time-reversal symmetry is lifted, we have to calculate $t_{\sigma',\sigma}$ for $\sigma = \uparrow$ and $\downarrow$ respectively.

With an external voltage applied $V \neq 0$, the system is in the nonequilibrium state, and it is usually dealt with via the Keldysh Green function approach, but in the present paper, we treat the nonequilibrium transport through this noninteracting electronic system via a method similar to that adopted to calculate the conductance in the preceding paragraph. Three basic assumptions are taken:

(i) at time $-\infty$, the ring and leads are not connected, and the two leads are in their own thermal equilibrium with the chemical potential $\pm V/2$;
(ii) the adiabatic switching on of the hopping parameters connecting the ring and leads yields a steady electronic flow at time 0 leaving the electronic distribution functions in the leads unchanged; and
(iii) in the tunnelling process, the electronic coherence is kept and its energy is conserved.

Under these assumptions, the wavefunction of an electron with energy E in lead l has the same form as that in the equilibrium state except that the wavevector k_l is related to E as $V_l - 2t\cos k_l = E$. By solving the corresponding Schrödinger equation, we can obtain $|t_{\sigma',\sigma}|^2$ and $|a_{n\sigma',\sigma}|^2$ at energy E. Then the current formula is

$$J = \int \sum_{\sigma',\sigma} |t_{\sigma',\sigma}|^2 \frac{\sin k_\mathrm{R}}{\sin k_\mathrm{L}} \,\mathrm{d}E \tag{8}$$

with $T_{\sigma',\sigma}(E) = |t_{\sigma',\sigma}|^2 \frac{\sin k_\mathrm{R}}{\sin k_\mathrm{L}}$ the transmission coefficient at energy E. In this Landauer–Büttiker formula, the integration is taken in the range from $\max\{E_\mathrm{F} - V/2, -2t + V/2\}$ to $\min\{E_\mathrm{F} + V/2, 2t - V/2\}$ because of the Pauli exclusion principle. This formula is in the same form as that derived from the Keldysh Green function approach at zero temperature. In the equilibrium state with $V = 0$, no extra spin is accumulated on the ring, and the spin accumulation comes entirely from the nonequilibrium unpolarized electronic current. Based on this consideration, the spin accumulation on the ring can be calculated as

$$S^v(n) = \sum_{\sigma'l\sigma'\sigma} \int \left(a_{n\sigma'l,\sigma}^\dagger \hat{\tau}_{\sigma'l\sigma'}^v a_{n\sigma',\sigma} \right) \mathrm{d}E \tag{9}$$

with the integration carried out in the same range as in J.

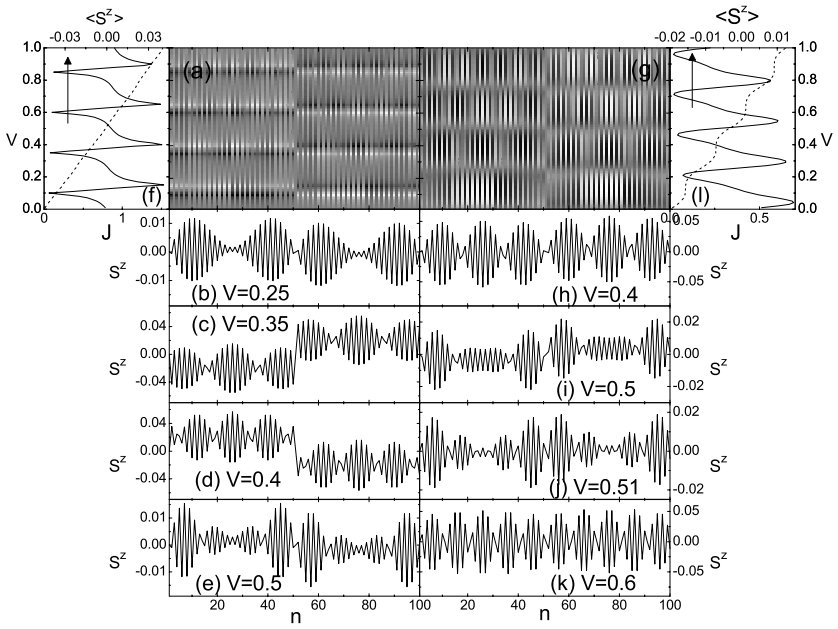

Figure 2. ((a) and (g)): Grey-scaled diagrams of the variations of S^z with V and n. (b)–(e) and (h)–(k): S^z–n curves at $V = 0.25$ (b), 0.35 (c), 0.4 (d), 0.5 (e), 0.4 (h), 0.5 (i), 0.51 (j) and 0.6 (k). (f) and (l): $\langle S^z \rangle$–V (solid) and J–V (dashed) curves. In (a)–(f), $Q_R = 0.6$, and in (g)–(l), $Q_R = 2$. In this figure, $E_F = -0.05$, and the other parameters are the same as in figure 1.

3. Results and discussion

In the calculations in this paper, we always set $t = 1$ and $N = 100$. As a comparison with the results of other authors [25–29], the variations of G in the equilibrium state are presented in figure 1(b), where the G–Q_R curves are illustrated at different E_F. Here, $Q_R = \frac{N t_{SO}}{\pi t}$, which has several physical meanings. It is the spin precession angle over the circumference of a 1D ring and is also the ratio between the perimeter and the spin precession length. According to an exact analytic expression derived from the effective mass Hamiltonian [25–28], G can be written as $G = g_0(k_F, \Delta_{AC})(1 - \cos \Delta_{AC})$ with k_F the Fermi wavevector and $\Delta_{AC} = \pi\sqrt{Q_R^2 + 1}$ the half of the difference between the phases accumulated by spin-↑ and spin-↓ electrons. Consequently, at $Q_R = \sqrt{Z^2 - 1}$ with Z an even integer, $G = 0$, which is caused entirely by the spin-sensitive quantum interference and independent of the specific value of E_F. However, the factor g_0, influenced by the back-scattering at the interfaces between leads and the ring, is dependent on E_F. All of these characteristics are verified by our numeric results. The small deviation of the zero positions from $\sqrt{Z^2 - 1}$ is due to the difference between the discrete and continuum models. Now we turn our attention to the nonequilibrium state and investigate the characteristics of the spin accumulation on this 1D Rashba ring.

The variations of S^z with V are presented in figures 2 and 3 at $E_F = -0.05$ and -1.8, respectively. In these two figures, the left half of the diagrams corresponds to the situation with $Q_R = 0.6$, and the right to $Q_R = 2$. We focus our attention on figure 2 and consider the former situation first. Figure 2(a) is a grey-scaled diagram of S^z–V–n, with S^z ranging from -0.06 (black) to 0.06 (white). A series of plateaus can be found, where the variation of S^z with V is slow at any specific site n, and between two successive plateaus a transitional region appears,

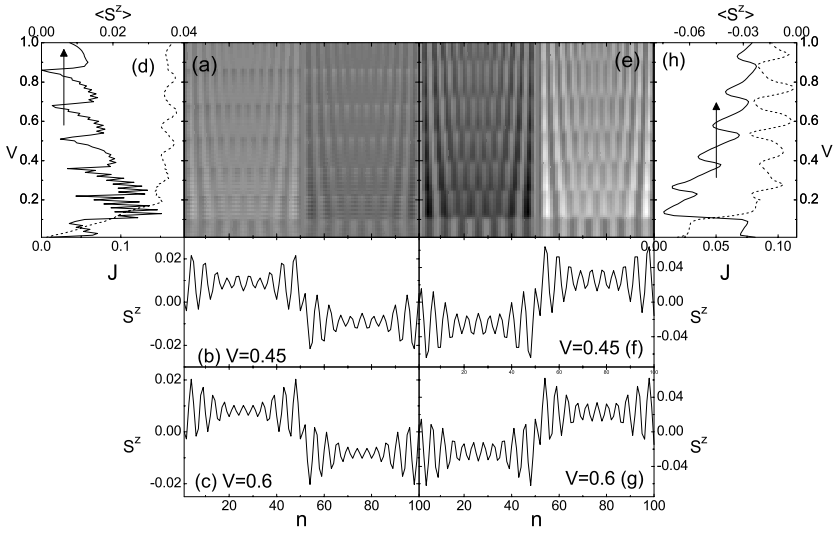

Figure 3. ((a) and (e)): Grey-scaled diagrams of the variations of S^z with V and n. ((b), (c), (f) and (g)): S^z–n curves at $V = 0.45$ ((b) and (f)), and 0.6 ((c) and (g)). ((d) and (h)): $\langle S^z\rangle$–V (solid) and J–V (dashed) curves. In (a)–(d), $Q_R = 0.6$, and in (e)–(h), $Q_R = 2$. In this figure, $E_F = -1.8$, and the other parameters are the same as in figure 1.

where S^z varies rapidly. The S^z–n curves are plotted in figures 2(b)–(e) at four specific values of V with (b) and (e) corresponding to V in two successive plateaus and (c) and (d) to the transitional region between them. These curves contain two types of oscillation: one is fast and the other slow. The beating pattern in the variation of S^z with n is remarkable at $E_F = -0.05$, close to the band centre. In the plateaus, every beating periods in the envelope function of S^z–n curve is complete, whereas in the transitional regions, new incomplete periods appear. In the situation with $Q_R = 2$, the variation of S^z with V has similar characteristics to those with $Q_R = 0.6$, and the beating pattern can even be seen directly from diagram (g), which is plotted in the same scale as figure 2(a).

In the experiments of present stage, only the average spin accumulation is measured, and we define

$$\langle S^z\rangle = \frac{2}{N}\sum_{n=2}^{N/2}\left(S^z(n) - S^z(n+N/2)\right) \tag{10}$$

as the average spin accumulation on the ring. In figures 2(f) and (l), the $\langle S^z\rangle$–V curves are plotted with $Q_R = 0.6$ and 2, respectively. Both of them contain a series of smooth plateaus, which have one-to-one correspondence with those in the S^z–V–n diagram. In the transitional regions, $\langle S^z\rangle$ changes rapidly and can even undergo a variation from negative to positive values, i.e., the accumulated electrons on the upper arm are changed from spin-↓ to spin-↑. These results are concerned with the out-of-plane spin accumulation. As in references [10] and [17], S^x also exhibits opposite signs on the two arms because of the precession of the spin-↑ and spin-↓ electrons in this Rashba ring. A similar plateau structure and beating pattern can be found in S^x, and its results are not presented here.

Obviously, the beating pattern in spin accumulation should affect the nonequilibrium electronic current. As can be seen from figures 2(f) and (l), the increase of J in the range $V < E_F + 2$ is not linear but has a series of plateaus—with complete beating periods formed on the ring, the increase of J with V is slow, whereas in the transitional regions J increases

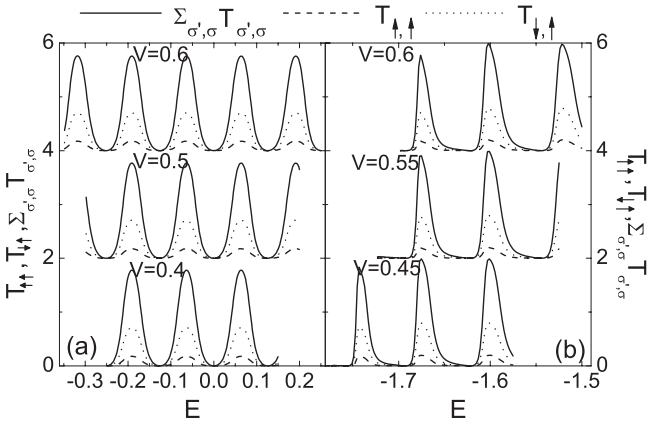

Figure 4. Variation of $T_{\uparrow,\uparrow}$ (dashed), $T_{\downarrow,\uparrow}$ (dotted) and $\sum_{\sigma',\sigma} T_{\sigma',\sigma}$ (solid) with E for $Q_R = 2$ at $E_F = -0.05$ (a) and -1.8 (b). From bottom to top, each set of curves is offset by two units. The other parameters are the same as in figure 1.

rapidly. This characteristic is more remarkable for $Q_R = 2$, and for $Q_R = 0.6$ it can still be found by checking the derivative variation of the corresponding J–V curve. If $V > E_F + 2$, the width of the transmission window in equation (8) is no longer increased, and the saturation of J is reached. Of course, this point cannot be reached in the considered range of V at $E_F = -0.05$.

In the three preceding paragraphs, we discussed the nonequilibrium results obtained at $E_F = -0.05$. As a comparison, figure 3 illustrates those at $E_F = -1.8$, which show the same characteristics. But with the Fermi energy close to the band edges, the distinction between the fast and slow oscillations in S^z–n curves is not clear, and the plateaus correspond to the situation where every oscillation period in the S^z–n curve is complete, and with a new period appearing, the system is in a transitional region. At $V = 0.2$, the transmission window reaches its maximum width. As V is further increased, the width remains unchanged, but this does not mean that J should also remain unchanged. Instead, J oscillates with small amplitude, accompanying the alternative variation of S^z between plateaus and transitional regions. With V increased, no direction reversal of $\langle S^z \rangle$ can be found in this situation.

To clarify the mechanism leading to the beating pattern and plateau structure, in figure 4, the $T_{\sigma,\uparrow} - E$ and $\sum_{\sigma',\sigma} T_{\sigma',\sigma} - E$ curves at different V are illustrated in the transmission window, where a series of spin-dependent resonant peaks can be found. When every peak in the window is complete, all of the beating periods in an S_z–n curve are complete also, and the system is in a plateau. If the peak–valley contrast is large, the difference between plateaus and transitional regions is distinct. For $E_F = -0.05$ (see figure 4(a)) with V increased, the window becomes wider and more peaks enter, whereas for $E_F = -1.8$, close to the band edges (see figure 4(b)) with $V > 0.2$, the width of the transmission window is no longer increased, but its position still moves with V. In this process, new peaks may enter the window, and old ones may leave, which leads to the plateau structure in the variation of S^z with V and the small oscillation of J–V curves.

For an isolated ring without Rashba SO coupling, there are N discrete states with $k_i = 2\pi i/N$. With ideal leads connected via tunnelling matrix elements, these states are perturbed, but N discrete resonant states can still be found in the structure, and tunnelling through these states results in a plateau structure in the nonequilibrium current. These perturbed states are no longer pure plane waves but are modulated because of the scattering at the interfaces, and

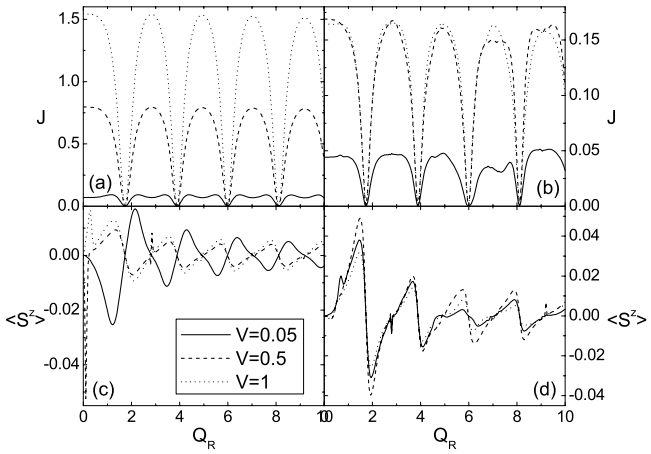

Figure 5. Variations of J ((a) and (b)) and $\langle S^z\rangle$ ((c) and (d)) with Q_R for $V = 0.05$ (solid), 0.5 (dashed) and 1 (dotted) with $E_F = -0.05$ ((a) and (c)) and -1.8 ((b) and (d)). The other parameters are the same as in figure 1.

closer to the band centre, the wavefunction beats more clearly. In a spin-symmetric ring, the resonant states are spin-independent and no spin can be accumulated. In a ring with $t_{SO} \neq 0$, at a specific energy, there are four spin-dependent wavefunctions corresponding to $\pm(k \pm k_{SO})$ with $k_{SO} = \frac{\pi}{2L_{SO}}$. The scattering at the interfaces modifies the unperturbed states and leads to beating in these spin-dependent resonant states. As in the spin-symmetric case, with E closer to the band centre, the beating pattern is clearer. As an evidence of spin Hall effect, spin accumulation can be found, which is an additive result. Careful checking of numeric data shows that the main contribution to S^z comes from the outmost unpaired resonant state in the transmission window and symmetric pairs with $E = 0$ cancel each other exactly. All of these lead to the beating pattern in the variation of S^z, which is a special property of a 1D mesoscopic Rashba ring. The results in the present paper are obtained at zero temperature, but only if the temperature cannot blur those resonant peaks can the beating pattern and plateau structure be found in a 1D Rashba ring.

In the preceding studies on the nonequilibrium state, two different Q_R values are taken: one is 0.6 and the other 2. How about the results with other Rashba SO coupling? In figures 5(a) and (b), the variations of J with Q_R are plotted for different V at $E_F = -0.05$ and -1.8, respectively. For any V and E_F, these curves oscillate quasi-periodically and have zeros at $Q_R \sim \sqrt{Z^2 - 1}$ with Z an even integer because of the AC effect and irrelevance of the positions of transmission zeros with the electronic energy in a pure 1D ring. For $E_F = -1.8$, the J–Q_R curve at $V = 0.5$ is close to that at $V = 1$, because in this situation the current has already been saturated. The variation of S^z with Q_R at different V is also calculated. In a grey-scaled diagram of S^z–Q_R–n, a specific beating pattern, independent of Q_R, can be found in the variation of S^z with n. At each site, S^z oscillates quasi-periodically with Q_R synchronously. We do not present this diagram, but give the $\langle S^z\rangle$–Q_R curves in figures 5(c) and (d). They oscillate quasi-periodically and have zeros at $Q_R \sim \sqrt{Z^2 - 1}$, which is also the consequence of spin-sensitive quantum interference. For $E_F = -0.05$, with $V = 0.05$ and 0.5, the oscillations of the $\langle S^z\rangle$–Q_R curves have a phase shift of π, resulting from the direction reversal of $\langle S^z\rangle$ with V. Although the main results of this paper are obtained at $Q_R = 0.6$ and 2, they can be looked at as two representatives in one quasi-period, and their basic characteristics can be found for any Q_R.

4. Summary

In summary, we investigate the nonequilibrium spin accumulation on a 1D mesoscopic Rashba ring with unpolarized current injected through ideal leads. Because of the spin Hall effect and back-scattering at the interfaces between the leads and the ring, a beating pattern can be found in the S^z–n curves. When every beating period in the envelope function is complete, a plateau is formed, where the variations of S^z, $\langle S^z \rangle$ and J with V are slow. If new incomplete beating periods enter the envelope function, a transitional region appears between two successive plateaus. This plateau structure and the beating pattern are related to the tunnelling through the spin-dependent resonant states in the nonequilibrium transmission window. Due to the AC effect, $\langle S^z \rangle$ and J oscillate quasi-periodically with Q_R, and exhibit a series of zeros at the same positions. In some situations, the direction of $\langle S^z \rangle$ can be reversed by V in this ring structure.

Acknowledgments

The author acknowledges the support by National Foundation of Natural Science in China Grant No 10204012, and by the special funds for Major State Basic Research Project No G001CB3095 of China.

References

[1] Prinz G A 1998 *Science* **282** 1660
[2] Awschalom D, Loss D and Samarth N (ed) 2002 *Semiconductor Spintronics and Quantum Computation* (Berlin: Springer)
[3] Zutic I, Fabian J and Das Sarma S 2004 *Rev. Mod. Phys.* **76** 323
[4] D'yakonov M I and Perel V I 1971 *JETP Lett.* **13** 467
[5] Hirsch J E 1999 *Phys. Rev. Lett.* **83** 1834
[6] Murakami S, Nagaosa N and Zhang S-C 2003 *Science* **301** 1348
Murakami S, Nagaosa N and Zhang S-C 2004 *Phys. Rev.* B **69** 235206
[7] Sinova J, Culcer D, Niu Q, Sinitsyn N A, Jungwirth T and MacDonald A H 2004 *Phys. Rev. Lett.* **92** 126603
[8] Rashba E I 1960 *Fiz. Tverd. Tela (Leningrad)* **2** 1224
Rashba E I 1960 *Sov. Phys. Solid State* **2** 1109 (Engl. Transl.)
[9] Shen S-Q 2005 *Phys. Rev. Lett.* **95** 187203
[10] Nikolic B K, Zarbo L P and Welack S 2005 *Phys. Rev.* B **72** 075335
[11] Kato Y K, Myers R C, Gossard A C and Awschalom D D 2004 *Science* **306** 1910
[12] Wunderlich J, Kaestner B, Sinova J and Jungwirth T 2005 *Phys. Rev. Lett.* **94** 047204
[13] Rashba E I 2004 *Phys. Rev.* B **68** 241315
Rashba E I 2004 *Phys. Rev.* B **70** 161201
[14] Inoue J I, Bauer G E W and Molenkamp L W 2004 *Phys. Rev.* B **70** 041303
Inoue J I, Bauer G E W and Molenkamp L W 2004 *Phys. Rev.* B **70** 161201
[15] Mishchenko E G, Shytov A V and Halperin B I 2004 *Phys. Rev. Lett.* **93** 226602
[16] Ma X, Hu L, Tao R and Shen S-Q 2004 *Phys. Rev.* B **70** 195343
[17] Nikolic B K, Souma S, Zarbo L P and Sinova J 2005 *Phys. Rev. Lett.* **94** 046601
[18] Zhang S and Yang Z 2005 *Phys. Rev. Lett.* **94** 066602
[19] Hankiewicz E M, Molenkamp L W, Jungwirth T and Sinova J 2004 *Phys. Rev.* B **70** 241301
[20] Sheng L, Sheng D N and Ting C S 2005 *Phys. Rev. Lett.* **94** 016602
[21] Nikolic B K, Zarbo L P and Souma S 2005 *Phys. Rev.* B **72** 075361
[22] Meijer F E, Morpurgo A F and Klapwijk T M 2002 *Phys. Rev.* B **66** 033107
[23] Aronov A G and Lyanda-Geller Y B 1993 *Phys. Rev. Lett.* **70** 343
[24] Qian T-Z and Su Z-B 1994 *Phys. Rev. Lett.* **72** 2311
[25] Datta S and Das B 1990 *Appl. Phys. Lett.* **56** 665
[26] Molnar B, Peeters F M and Vasilopoulos P 2004 *Phys. Rev.* B **69** 155335
[27] Frustaglia D and Richter K 2004 *Phys. Rev.* B **69** 235310
[28] Souma S and Nikolic B K 2004 *Phys. Rev.* B **70** 195346
[29] Souma S and Nikolic B K 2005 *Phys. Rev. Lett.* **94** 106602